STUDY ABOUT THE TECHNICAL VIABILITY OF USING COMPOSITE MATERIALS IN THE REHABILITATION OF HYDRAULIC/AGRICULTURAL HIGHWAY UNDERPASSES.

Miguel Maria Potes Barroso Silva Santos
miguelsilvsantos@tecnico.ulisboa.pt

Instituto Superior Técnico, University of Lisbon, Portugal (2020)

Abstract

Since the 1980´s until the beginning of this XXI century, a constructive solution based on corrugated steel sheets, generally known as the ARMCO solution, was extensively adopted in the construction of highways to execute hydraulic (PH) and agricultural (PA) highway underpasses. Less than 30 years after their construction the level of corrosion was found to be higher than expected. Such corrosion directly influences the steel strength and can compromise the safety of these structures. This problem has already caused serious road subsidences in Portugal. Therefore, it is urgent to develop rehabilitation solutions for these PH/PA, some of which have a diameter of about 4 m. One of these solutions, which has already been applied by highway operators, consists of using Glass Fiber Reinforced Polymer (GFRP) pipes in the inner soffit of the existing steel pipes. However, some doubts have been raised about the technical viability of this new structural solution, mainly due to the lack of knowledge about the structural behavior of composite materials for this specific type of rehabilitation. The objective of this dissertation was to evaluate the technical viability of rehabilitating PH/PA using GFRP pipes, namely their application in the inner soffit of the old steel pipe. To fulfil this objective, an experimental and numerical study was developed, which focused on a commercially available GFRP pipe, already used in this type of rehabilitation. To understand how this GFRP solution is executed, an example of a rehabilitation work of a PH located in the Portuguese motorway A33, in Sarilhos Grandes, is presented. Overall, despite the lack of information about the long-term performance of this solution, this study allowed concluding that the use of GFRP pipes in PH/PA rehabilitation is technically viable.

Keywords: Hydraulic underpasses; ARMCO; Corrugated steel sheets; Corrosion; Rehabilitation; Composite materials; GFRP; Laboratory tests; Finite element simulation; Field study.

1. Introduction

Since the 1980s until the beginning of this XXI century, during the expansion of Portuguese highways, it was necessary to construct many hydraulic and agricultural underpasses; in many of these projects, a construction system called ARMCO solution was adopted. This system consists of using corrugated steel sheets, with an average thickness between 4 and 7 mm, which are screwed together, being assembled *in situ* before landfilling (Figure 1a).

Although the ARMCO solution has been extensively used, not only in Portugal but in many other countries, a few years after their construction, well before their service life was reached, the level of corrosion in these structures was found to be higher than expected, sometimes even compromising the safety of the PH/PA and the overlying track.

Since 2016, there have been three road subsidences in Portugal due to the loss of mechanical resistance of PH/PA built with the ARMCO solution, caused by the corrosion of those metal pipes. Figure 1b shows the subsidence that occurred in the Portuguese motorway A41, which created traffic interruptions for months. The most serious case to date occurred in 2013, when the collapse of a national road in Poland caused two deaths.

Figure 1 – a) Example of the ARMACO solution; b) Road subsidence in A41 (2016) Portugal [1].

Considering that there are numerous passages of this type, built at approximately the same time, it is imperative to find a technically viable rehabilitation solution, in terms of strength and stiffness, easy and quick to apply (without creating constraints on the overlying traffic), which is economically viable, durable and corrosion-resistant.

In recent years, PH/PA in ARMCO have been rehabilitated with various solutions, including conventional technologies with traditional materials, such as reinforced concrete and steel. These solutions present some constraints or limitations associated with the constituent materials' intrinsic characteristics and/or their application process [2].

As a result, there has been a growing interest from road infrastructure management authorities in the application of Glass Fiber Reinforced Polymer (GFRP) pipe for such rehabilitation works. This solution, which is explained in detail in this extended abstract, consists in applying a GFRP pipe in the inner soffit of an old steel pipe. The empty space between the steel and the GFRP pipes is then filled with grout, connecting these two components into a single part. To study the technical viability of this rehabilitation solution, an experimental and numerical study was developed, which was complemented by a field study of a rehabilitation work in A33 motorway.

Since there are no international standards yet available for the design of this type of rehabilitation with GFRP composites, and these materials can present a significant variation in their geometry and composition, the first part of the assessment of their technical viability included an experimental study about their mechanical properties and structural behaviour.

The experimental program was divided into two parts: (i) mechanical tests for the characterization of the GFRP material (bending, compression, in-plane shear, and interlaminar shear); and (ii) flexural tests in full-scale GFRP pipes, with a wall thickness of 54 mm, 3540 mm of opening, and 2200 mm of height The experimental tests allowed the evaluation of the mechanical properties of the GFRP material (elastic moduli and strength) as well as the structural behavior and load capacity of the full-scale pipes.

The numerical study, developed using a commercial finite element (FE) software, was also divided into two parts: (i) simulation of the structural behavior of the full-scale GFRP pipes tested in flexure; and (ii) simulation of a generic PH construction considering the interaction between the GFRP pipes, the landfill soil, and the lanes – this aimed at checking whether this rehabilitation solution fulfils applicable structural safety requirements.

Finally, to understand how this GFRP solution is executed, it will be presented one example of a rehabilitation work of a PH located in the Portuguese motorway A33, in Sarilhos Grandes. The possibility to assess this rehabilitation project *in situ* clearly showed the advantages of this constructive solution: simplicity and execution speed.

2. Experimental Study

2.1 Physical and mechanical tests

Fiber content

The fiber content was determined according to the experimental procedure described in ISO 1172 [3]. The test consists of separating the different components of the composite material through (i) the calcination of the polymeric resin by heating; and (ii) the subsequent separation of the glass fibers and the filler by sieving. After the separation and successive weighing, it is possible to obtain the mass content of the different components that make part of the composite material used in the tubular elements, namely, the polymeric polyester resin, the filler (quartz sand), and the glass fibers. The results obtained are summarized in Table 1.

Table 1 – Fiber content tests results

Specimen	TF-1	TF-2	Average
Polymeric resin mass content (%)	43.5	43.5	43.5
Filler mass content (%)	30.9	30.6	30.8
Fiber glass mass content (%)	26.6	26.8	26.7

Flexural Tests

Flexural tests were performed in 3 specimens (F1 to F3) according to EN ISO 14125 [4], following method A (three-point bending). According to this method, the specimens' dimensions depend on the material class, which in this case is class III. These dimensions (1800x54x120 mm) and the adopted span (1200 mm) caused failure to occur by tension/compression of the lower/upper fibers, while avoiding rupture due to interlaminar or in-plane shear (Figure 2).

To study the heterogeneity of the material and the influence of the specimens' curvature, one of the specimens (F3) was tested with the concavity facing downwards (the result being presented as F3i) and, later, with the curvature facing upwards (such as in specimens F1 and F2). In the first test, the specimen was subjected to a low force to ensure that no damage would occur.

The ultimate stress ($\sigma_{fu,x}$) and strain ($\varepsilon_{fu,x}$) and the flexural modulus ($E_{f,x}$) in the longitudinal direction were obtained through the formulas presented below. The results obtained are shown in Table 2.

$$\sigma_{fu,x} = \frac{3 \times F_u \times L}{2 \times b \times h^2}$$

$$\varepsilon_{fu,x} = \frac{6 \times \delta_u \times h}{L^2}$$

$$E_{f,x} = \frac{L^3}{4 \times b \times h^3} \times \left(\frac{\Delta F}{\Delta s}\right)$$

F_u – Ultimate load;
b – specimen width;
h – specimen height;
L – Test span (1200 mm);
δ_u – Displacement at the mid-span section at failure;
$\Delta F/\Delta s$ – slope of the load vs displacement curve.

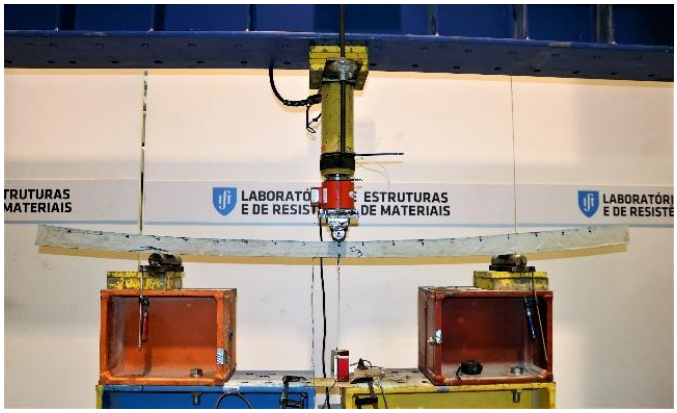

Figure 2 – Flexural test (F3).

Table 2 – Flexural test results.

Property	F1	F2	F3	Average	Coefficient of variation [%]	F3i
F_u [kN]	58.1	63.7	66.4	62.7	6.75	*
$\sigma_{fu,x}$ [MPa]	334	307	306	316	5.03	*
K [kN/mm]	0.53	0.65	0.67	0.62	12.21	0.62
$E_{f,x}$ [GPa]	15.2	14.1	14.1	14.5	4.4	14.5
$\varepsilon_{fu,x}$ [μm/m]	21746	20380	19557	20561	5.38	*
* - Specimen F3i was not tested up to failure.						

Figure 3 depicts the stress *vs.* strain curves, showing a notable similarity between the slope of the various curves/specimens.

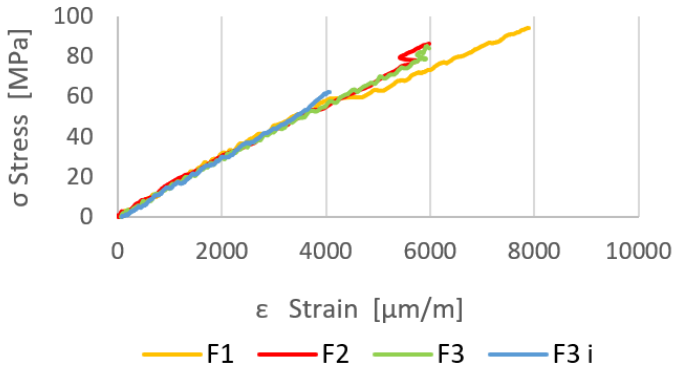

Figure 3 – Flexural tests: stress vs. strain curves.

Interlaminar Shear Tests

The objective of the interlaminar shear test, which was carried out according to ISO 14130 [5], was to determine the shear resistance of the matrix layer between the fibre reinforcement layers. To this end, 5 specimens with dimensions of 600x120x60 mm were subjected to a single load applied at the centre of a 300 mm short span. The relationship between the thickness and the span was set (based on the above-mentioned standard) to cause the rupture by delamination of the layers. Figure 4 shows the load *vs.* midspan displacement curves in the longitudinal direction – the average interlaminar shear strength obtained in these tests was $\tau_x = 14.9$ MPa (coefficient of variation of 4.9%).

In the transverse direction (y), it was not possible cause interlaminar shear failure, as specimens failed due to (transverse) tension of the lower fibers. These tests allowed to determine the average tensile strength in the transverse direction, $\sigma_{tu,y} = 90.7$ MPa (coefficient of variation of 2.6%).

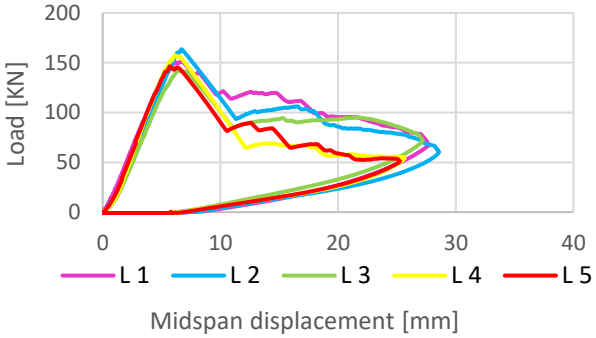

Figure 4 – Interlaminar shear tests: load vs. midspan displacement curves of longitudinal specimens.

Compression Tests

The compression tests were performed according to the D 695 standard [6] along the two main directions to determine the elasticity moduli in compression, $E_{c,x}$ and $E_{c,y}$, the maximum compressive stresses, $\sigma_{cu,x}$ and $\sigma_{cu,y}$, and the respective strains $\varepsilon_{cu,x}$ and $\varepsilon_{cu,y}$.

Table 3 shows a summary of the compression test results. The mean value for the maximum longitudinal compressive stress ($\sigma_{cu,x}$) was 211 MPa. As expected, the ultimate stress in the transverse direction ($\sigma_{cu,y}$) was lower, with an average value of 107 MPa. This difference reflects the orthotropy of the GFRP material, with the compressive strength in the longitudinal direction being approximately twice than the strength in the transverse direction. A similar difference was verified between the elasticity moduli in the longitudinal (14 GPa) and transverse directions (6 GPa).

Table 3 – Compression test results.

Propertie		Longitudinal (x)	Tansversal (y)
$E_{c,x}$ [GPa]	Average	14.00	5.96
	Var. Coef. [%]	14.23	2.81
F_u [kN]	Average	273	139
	Var. Coef. [%]	6.57	16.93
$\sigma_{cu,x}$ [MPa]	Average	211	107
	Var. Coef. [%]	4.72	16.84
$\varepsilon_{cu,x}$ [μm/m]	Average	13206	18907
	Var. Coef. [%]	19.30	17.32

2.2 Full-scale test

The full-scale tests were performed on three specimens (PH1, PH2, PH3, Figure 5) with an ovoid-shape, with 1 m of length, a maximum opening of 3540 mm and a height of 2200 mm. The test consisted in applying a transverse load at the top of the GFRP tube – using a hydraulic jack with a 600 kN capacity and with a 250 mm stroke – by means of a steel load distribution beam. The test specimens have typical dimensions of GFRP tubular elements used in PH/PA rehabilitation.

The main purpose of the full-scale tests was to evaluate the structural behaviour of these pipes when loaded in flexure, by assessing the strains (stresses) and displacements in different locations. These tests also allowed to assess the accuracy of the FE models used in the numerical study, namely their accuracy in predicting the deformability and the load capacity of the tubular elements. Because the specimens had a very big (and unusual) size and relatively high flexibility, it was necessary to introduce a few changes in the setup from the test of specimen PH1 to the test of specimens PH2 and PH3.

The PH1 specimen was supported in a mortar layer along a width of 2.1 m; no additional restrictions were applied to this specimen, namely to prevent the lateral displacements in other cross sections; due to these (relatively flexibe) supporting conditions, it was not possible to cause failure of this specimen (also due to the low elastic moduli of the GFRP material). To increase the structural stiffness, in the tests of specimens PH2 and PH3, a mechanism was used that restricted the lateral movements in the cross-sections where the pipes have their maximum opening. With this mechanism, which is displayed in Figure 5 (comprising two steel beams and dywidag anchors), it was possible to cause failure of specimens PH2 and PH3.

Figure 5 – Full-scale test (PH2).

In the test of specimen PH1, besides the inability to cause specimen failure, there were also some uncertainties related to the support conditions, which were found to change during the test – in fact, the mortar layer cracked and fractured during the tests. Yet, it was possible to obtain relevant data in this.

Figure 6 shows the load vs. vertical displacement at the top (D1) of specimen PH1. It can be verified that the maximum stroke of the hydraulic jack (250 mm) has been reached at a 200 kN load, without causing specimen faiure. After an initial phase in which the behavior was non-linear, the structure presented a linear elastic behavior, with a proportional increase of the deformation with the load increase. After the maximum stroke of the jack was attained, the tubular element was unloaded and largely recovered its initial position. At the end of the unloading stage, the residual deformation was about 5%, corresponding to a permanent vertical displacement at the top of the specimen of 13 mm, which should be essentially associated with the aforementioned damage in the support layer. These results prove, once again, the high elasticity of the GFRP material.

The load vs. displacement (D1) curves of specimens PH2 and PH3 also showed a linear behavior practically until their failure, similarly to specimen PH1. The failure of specimen PH2 occurred for a load of 371 kN, corresponding to a displacement D1 of 162 mm – failure occurred with a load force reduction and displacement D1 increase. For a load of 200 kN, the displacement D1 in PH1 specimen was 240 mm, while in PH2 specimen such displacement was 80 mm – this reflects the remarkable stiffness increase (3 times) provided by the lateral support system used in the tests of specimens PH2 and PH3. Specimen PH3 presented a similar behavior to specimen PH2. However, the slope of the curve of specimen PH3 is higher than that of specimen PH2, reflecting a higher stiffness (25%) of the former specimen. This stiffness difference is consistent with the difference in ultimate strength, which was also higher in specimen PH3 (464 kN) than in specimen PH2 (371 kN).

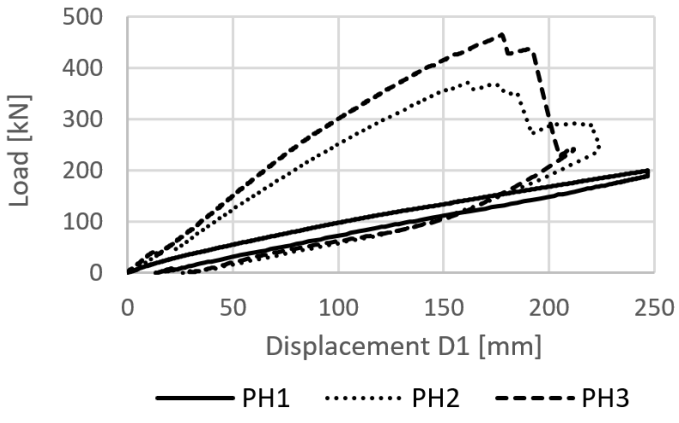

Figure 6 – Full-scale tests: Load vs. Displacement curve.

Since the weight of specimens PH2 and PH3 was quite similar, the stiffness difference may be, at least in part, justified by differences encountered in the average wall thickness at the top of the pipe (9% higher in specimen PH3). This geometrical difference also explains the higher load capacity of specimen

PH3, which presented higher thickness at the critical (top) cross-section, where failure occurred. Note that for a uniform distribution of glass fibers throughout the section depth, the flexural strength depends on the section height's square; in this case, the square of the ratio between the thickness of specimens PH3 and PH2 in the central zone is 1.26, which practically matches the ratio between the maximum forces measured on those specimens (1.25).

Failure of specimens PH2 and PH3 occurred by compression (crushing) of the fibers on the upper surface of the top section of the tube, which was subjected to bending and compression (as detailed in the numerical study). After failure was triggered, the rupture by compression was followed by interlaminar shear failure, with delamination of the different layers, leading to an inclined crack (Figure 7). At some point, a hinge formed in this central part of the top of the tube. It was also possible to observe a longitudinal tensile crack along the bottom surface of the GFRP tube.

Figure 7 – Full-scale tests: interlaminar shear with delamination of the different layers.

Figure 8 shows the load vs. strain curves recorded in two pairs of strain gauges placed in the same zone of test specimens PH2 and PH3. Each pair of strain gauges was placed as follows: one was placed in the outer surface (recording tensile strains) and the other one on the inner surface (recording compressions strains) of the GFRP pipe, at a cross-section distanced 220 mm from the top section.

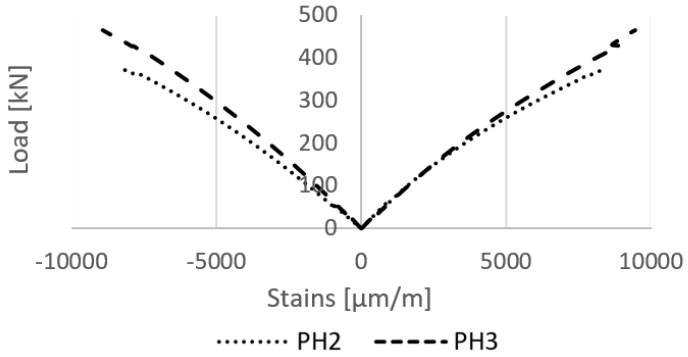

Figure 8 – Full-scale tests of specimens PH2 and PH3: Load vs. strain curves.

The maximum strain (at failure) in specimens PH2 and PH3 corresponded to an approximate compressive stress of 140 MPa (considering E = 14.5 GPa). Since these strain gauges were placed at a distance of 220 mm from the load application section, it was not possible to determine the maximum tension in that critical section (this was assessed based on the numerical models). For similar loads, the maximum strains recorded in specimen PH1 were considerably smaller than those measured in the other two specimens, due to the absence of lateral restrictions in the test of specimen PH1.

3. Numerical Study

The numerical study consisted of developing several models using the finite element program SAP2000 (SAP). The models were previously prepared in AutoCAD (ACAD) regarding the overall geometry. In this part of the study, two situations are analyzed: (i) a situation identical to the full-scale laboratory tests; and (ii) a simulation of a generic PH construction, in which the interaction between the GFRP pipes, the landfill soil, and the lanes were considered.

3.1 Simulation of full-scale tests

This main objective of the study were to develop a model capable of simulating the structural response of the full-scale pipes tested in the laboratory, predicting their stresses and deformations, and comparing the FE results with those measured in the tests. The model also aimed at obtaining a better knowledge of the properties and behaviour of this type of composite structure, namely to estimate its resistance; in fact, in the tests it was not possible to measure the maximum stresses in the loaded section.

The GFRP pipe was modelled using shell FEs as a linear elastic material, with the orthotropic properties measured in the characterization tests. A unitary load of 1 kN was applied in an area of 0.15 x 1 m^2 at the top of the pipe, as in the experimental test. This load corresponds to a uniformly distributed load (pressure) of 6.67 kN/m^2. Therefore, all the results obtained in this FE model depend on this unitary load.

As mentioned, the model was first prepared in ACAD. Based on a survey of the specimens' thickness, a constant nominal thickness of 60 mm was considered in the different sections. Once the geometry was defined, the GFRP material and respective section was assigned to these elements.

The support conditions, defined in the numerical model, were identical to the restrictions imposed in the experimental tests of the last two specimens (PH2 and PH3), in which vertical displacements were restricted in two horizontal alignments of the lower face. In addition, in the zone of the pipe with the

greatest width, the lateral movements were restricted by two springs. These springs were used to simulate the lateral restrictions imposed by the supports shown in Figure 9. The stiffness of these springs was (back) calculated based on the displacements measured in the laboratory tests. Consequently, the stiffness (k) of each of these supports (25 in each horizontal alignment) was defined as k = 1000 kN/m.

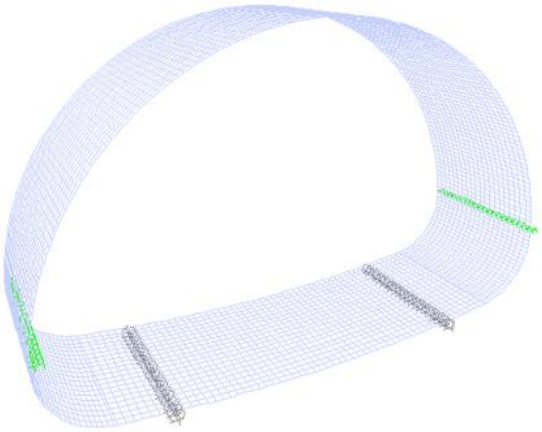

Figure 9 – Model simulated in SAP2000.

The stiffness of the structure obtained from the FE model was determined by dividing the 1 kN load by the displacement D1 at the top of the pipe. Figure 10 compares the initial load vs. displacement D1 curves measured in the tests of specimens PH2/PH3 and obtained from the FE model. Figure 10 shows that the stiffness obtained from the FE model is quite similar to the average stiffness from the two tests.

For a 40 kN load, the displacement obtained from the model was 14.2 mm. This displacement compares with an average experimental value of 13.6 mm – values measured in specimens PH2 and PH3 were respectively 15.6 mm and 11.6 mm. Note that the thicknesses of the GFRP pipe measured at the top of specimens PH2 and PH3 were 58 mm and 65 mm, respectively, and that the thickness considered in the FE model (60 mm) is intermediate between these two values. This may partly explain the fact that the numerically obtained stiffness is also intermediate between the stiffness values measured on both specimens.

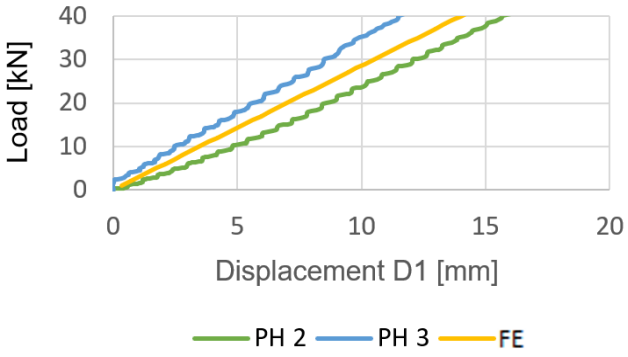

Figure 10 – Initial load vs. strain curves PH2/PH3 and FE.

Figure 11 compares the evolution of the axial strains with the applied load registered in strain gauges ext1 (compression) and ext2 (tension) of specimens PH2/PH3 with the corresponding strains calculated by the FE model. It is possible to see a good agreement between the numerical and experimental results.

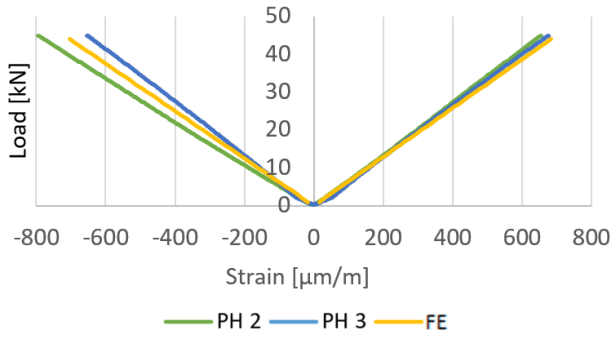

Figure 11 – Load vs. strain curves PH2/PH3 and FE.

Maximum axial stresses were found to develop in the upper cross-section of the specimens. In each section, compression stresses were always higher than the tensile ones (Figure 12). This is due to the fact that each section is subjected to a bending moment (which generates symmetric tensile and compression stresses in the extreme fibers) and an axial compression (which generates uniform compression stresses in the section depth).

The maximum stress obtained from the FE model for the unitary load was 500 kPa. For the maximum forces measured in the tests of specimens PH2 and PH3 (397 kN and 464 kN), the estimated failure stresses were 199 MPa and 203 MPa, respectively. These values compare well with the maximum compressive stress obtained in the laboratory tests (211 MPa).

The maximum shear stress for the unitary load, calculated by the FE model was 90 Pa, significantly lower than the interlaminar shear strength obtained in the interlaminar shear tests (127 kPa). Therefore, it was concluded that the contribution of shear stresses to the collapse mechanism was not very significant.

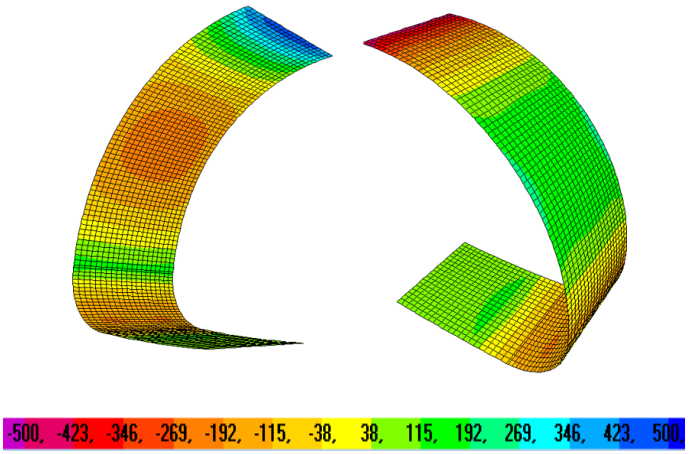

Figure 12 – Numerical axial stresses for the unitary load (kPa).

3.2 Simulation of a PH project situation

After the validation of the numerical models, a project situation was simulated. For that, a generic PH construction was modelled considering the interaction between the GFRP pipes, the landfill soil, and the lanes. The main objective of this simulation was to check if this rehabilitation solution meets applicable structural safety requirements.

A road with two lanes, one in each direction, was considered. Each of these lanes is 3 m wide and has an associated shoulder of 1 m. A walkway of 1 m wide was also considered on each side of the road. The landfill was placed at a level of 0.60 m above the pipe, corresponding to the minimum value used in this type of constructions. Solid (brick) finite elements were used to simulate the landfill. The composite material of the pipe and the bituminous pavement were simulated using shell elements. The GFRP pipe's thickness and stiffness were equal to those used in the previous model. The bituminous pavement was modelled with a thickness of 50 mm and an elastic modulus of 2.5 GPa, as an isotropic material The landfill and pavement properties were based on a study carried out at IST [7]. This three-dimensional model is shown in Figure 13.

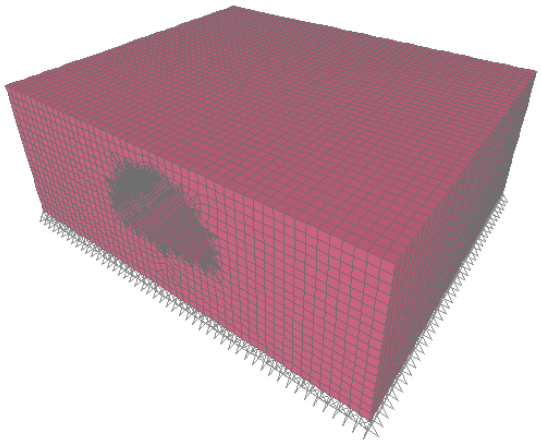

Figure 13 – Three-dimensional FE model used in the simulation of the project situation.

According to the Portuguese safety code for structures of buildings and bridges (RSA) [8], two different types of actions / combinations of actions should be considered in the design of this type of structures, in addition to the gravity loads (G), associated with the self-weight of the GFRP material, landfill and bituminous pavement:

(A) A load vehicle (Q_{LV}) with three axes with 2.0 m of width distanced 1.5 m apart (in the longitudinal direction), each one weighing 200 kN.

(B) The simultaneous effect of a uniformly distributed surface load of 4 kN/m^2 and a uniformly distributed linear load of 50 kN/m (Q_{DL}).

For both types of actions / combinations of actions, two alternative situations were considered: the vehicle or the linear load were placed (1) centred at the midspan of the hydraulic passage (to maximize stresses at the centre of the pipe); and (2) in a section 1.5 m apart from the midspan (to maximize stresses at the section of the pipe where its width is maximum).

After successive analyses (for the different positions of the loads), the maximum deformations and the maximum stresses were obtained (for different combinations of actions), considering both the gravity loads (nominal values) and the live loads (characteristic values). The maximum deformation obtained (δ_{max} = 9.2 mm) occurred in the top center of the pipe, corresponding to the linear uniformly distributed load of 50 kN/m applied above the midspan (Figure 14).

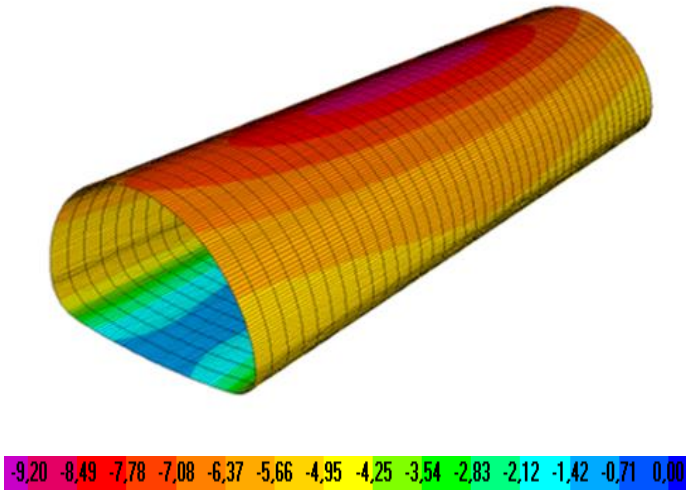

Figure 14 – Vertical displacements (mm) obtained for the load combination G+Q_{DL}-centred.

The maximum axial stress (σ_{max} = 9.5 MPa) was obtained for the combination (B), but this time with the linear load positioned at a distance of 1.5 m from the midspan (Figure 15).

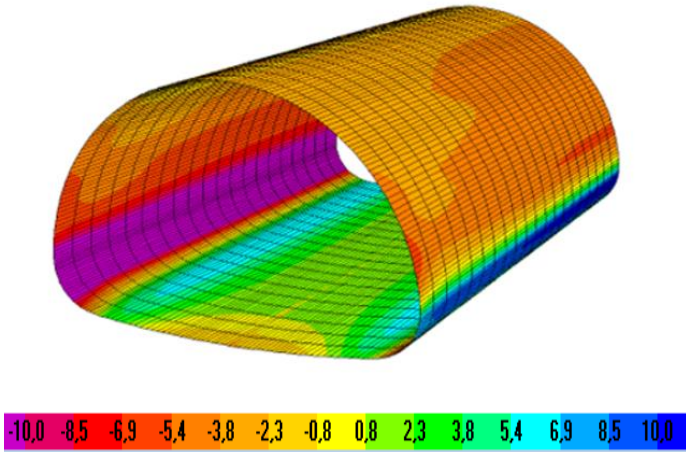

Figure 15 – Axial design stresses σ_{11} obtained for the load combination G+Q_{DL}-eccentric.

3.3 Safety verification

Serviceability Limit States (SLS) – To verify the fulfilment of long-term deformation requirements, it was necessary to take into account the creep effect in the calculation of deformations caused by permanent loads (self-weight); for this purpose, a creep coefficient (ϕ) of 0.68 was considered in the GFRP material (prCEN/TS 19101: 2020, Table 4.8) [9]. A conversion factor for environmental conditions (η) was also taken into account; in this case, because the structure will be potentially in permanent contact with water, the most unfavourable value was considered: $\eta = 0.6$ (prCEN/TS 19101: 2020, Table 4.6). The maximum deformation for the characteristic load combination was 14.0 mm. This value is lower than the limit of L/250 (= 14.2 mm), thus fulfilling the SLS safety requirement.

Ultimate Limit States (ULS) – Based on the maximum stresses obtained from the project situation simulation, safety checks were carried out to verifiy the fulfilment of ULS. These checks were carried out in accordance with the recent document prCEN/TS 19101: 2020 [9].

The design stress (σ_{Ed}) was calculated based on the characteristic values of the maximum stresses σ_{Ek} obtained from the FE project simulation. A load partial factor γ_i was assigned to each load (of the most unfavourable combination), depending on the type of action: for variable loads, such as the load vehicle and the uniformly distributed live loads, a load partial factor $\gamma_Q = 1.50$ was set; for permanent loads (gravity loads) a load partial factor $\gamma_G = 1.35$ was considered. Consequently, a design value of the maximum (compressive) stress $\sigma_{Ed} = 13.8$ MPa was obtained.

The design value of the compressive strength σ_{Rd} was obtained from the characteristic value of the compressive strength (σ_{Rk}), determined from the material characterisation tests, as per prCEN/TS 19101: 2020 [9]. To determine σ_{Rk}, a material partial factor (γ_m) was considered that takes into account the experimental variability (coefficient of variation $V_x = 4.7\%$, multiplied by a corrective factor $f_{Vx} = 1.70$ (5 specimens), resulting in $V_{x,exp} = 8.0\%$) of the material properties ($\gamma_m = 1.12$), as well as the conversion factor that reflects the environmental conditions that the material will be exposed to during its service life ($\eta_c = 0.6$).

Therefore, the characteristic value of the compressive strength was determined to be $\sigma_{Rk} = \sigma_{Rm} / \gamma_m = 211 / 1.12 = 188$ MPa; and the design value of the compressive strength was determined to be $\sigma_{Rd} = \sigma_{Rk} \times \eta_c / \gamma_{Rd} = 188 \times 0.6 / 1.4 = 81$ MPa.

Since the design value of the applied stress ($\sigma_{Ed} = 13.8$ MPa) is lower than the design value of the corresponding strength ($\sigma_{Rd} = 81$ MPa), the safety at ULS is verified.

These models showed that PH/PA rehabilitation with GFRP pipes meets the structural safety requirements for both ultimate limit states and serviceability limit state.

4. Rehabilitation Example

The rehabilitation work that was visited in the final part of this dissertation is located at the exit number 3 of the Portuguese motorway A33, Sarilhos Grandes (Figure 16a). Five parallel tubular structures, with an ovoid shape, were built in 1997 using the ARMCO solution. This structure was designed to ensure a flow of approximately 100 m^3/s, for a return period of 100 years, through the 5 parallel passages, each one being 30 m long. With the ARMCO structure, the maximum flow rate was 150 m^3/s. This value increased with the GFRP rehabilitation (due to the decrease of the roughness coefficient) to 200 m^3/s.

To proceed with this GFRP rehabilitation, some preliminary works are necessary. These depend not only on the state of conservation of the PH/PA, but also on the slope's state and the access to the existing tubes. Examples of preliminary works required in the vast majority of cases include deforestation of the slopes, diversion of water from the interior of the old steel pipe, removal of silted soils, and the general cleaning of the pipe to be rehabilitated. After receiving the GFRP tubes on-site, their geometry must be checked, and it must be confirmed that the tubes have not been damaged during transport.

The second step is to place the new pipes inside the degraded ones. For this, a longitudinal rail-like structure must be installed over which the tubes will move (Figure 16b). Then, the tubes are usually pushed to their final position with a mechanical winch. The tubes are connected through joints that depend on the supplier of the tubes. There are essentially two types of connections: (i) one that consists of a male-female connection, in which silicone is placed along the joint before fitting; and (ii) another one that is secured by two pipe flaps. In any case, the connection requires the greatest attention and control to ensure good performance of the joints. If such connections are not successfully executed, then this will likely be a source of pathologies in the future.

The third step starts by shoring the GFRP pipes to prevent them from moving due to the upward impulses caused by grout injection (to be applied later). After shoring all tubes, both pipe ends are buffered, and the grout injection is started. The grout injection must be done in a phased manner to ensure both homogeneity throughout the passage and uniformity of the lateral impulses. This is the most challenging stage (Figure 16c). Once the new GFRP piping is joined to the old one, some finishes are carried out, such as paintings, finishing details of the PH/PA enter/exit, and assembly of energy sinks upstream and/or downstream, depending on the needs. Figure 16d

shows the final stage, i.e. the state of the hydraulic passage once the GFRP rehabilitation is completed.

Figure 16a – Initial state of the PH after deforestation work.

Figure 16b – Installation of the GFRP pipes.

Figure 16c – GFRP pipes shored and buffered, ready to start the first stage of grout injection.

Figure 16d – PH after rehabilitation.

5. Conclusions

The following main conclusions are drawn from this study:

1. The material characterisation tests allowed assessing the constituent materials of the GFRP tubes and evaluating the mechanical properties of the material (elastic moduli and strength).

2. In the flexural full-scale tests, the GFRP pipes showed linear elastic behaviour almost up to failure, which occurred in a brittle way, and presented high deformability. The different specimens presented significant thickness variation, which influenced the structural behavior – this draws the to attention to the importance of quality control during the manufacturing process.

3. The numerical study showed that it is possible to simulate the structural behavior of GFRP pipes with accuracy by using conventional FE models. These models also showed that PH/PA rehabilitation with GFRP pipes allows fulfilling the structural safety requirements, for both ultimate limit states and serviceability limit states, even without considering the contribution of the existing structure and/or the grout connecting the new GFRP pipes to the old steel ones. Therefore, it is feasible not only to use this technology in rehabilitation works but also in new constructions of PH/PA.

4. With current construction techniques, it is possible to carry out this type of rehabilitation works with GFRP tubes with safety and quality. These rehabilitation solutions have two major advantages: (i) smaller companies can compete for this type of rehabilitation works more easily; and (ii) it does not promote market niches, dominated by the few companies that already control this technology – in other words, the construction technology is relatively straightforward.

Overall, despite the lack of information about the long-term performance of this solution, this study allowed concluding that the use of GFRP pipes in PH/PA rehabilitation is technically viable.

References

[1] Jornal de Notícias website: https://www.jn.pt/, accessed on 1 December 2020.

[2] A.T. Ferreira de Sousa (2018). Estudo de soluções de reforço de passagens hidráulicas construídas por perfis de chapas de aço corrugado. Dissertation to obtain the master's degree in Civil Engineering, Faculty of Engineering, University of Porto.

[3] ISO 1172 (1996) Determination of the Textile-Glass and Mineral-Filler Content – Calcination methods.

[4] EN ISO 14125 (1998). Fibre-Reinforced Plastic Composites - Determination of flexural properties.

[5] EN ISO 14130 (1998). Fibre-Reinforced Plastic Composites - Determination of Apparent Interlaminar Shear Strength by Short Beam Method.

[6] ASTM D695 (2002). Standard Test Method for Compressive Properties of Rigid Plastics.

[7] J.R. Correia; M.R.T. Arruda and F.A. Branco (2012). Structural Assessment of Reinforced Concrete Arch Underpasses Subjected to Vehicular Overloads, Journal of Performance of Constructed Facilities, Vol. 28, No. 2, pp. 321-329.

[8] Regulamento de Segurança e Ações de Edifícios e Pontes (1983).

[9] prCEN/TS 19101:2020. Technical Specification “Design of fibre-polymer composite structures”.